RESEARCH ARTICLE

BON VIEW PUBLISHING

Improvement of Read Performance Using CMOS on Array (COA) in 3D NAND Flash

Hyowon Kang[1] and Daewoong Kang[2],*

[1]*Department of Engineering, Korea International School, Republic of Korea*

[2]*Department of Next Generation Semiconductor Convergence and Open Sharing System, Seoul National University, Republic of Korea*

Abstract: 2D NAND flash cells were unable to continue scaling due to several physical limitations including few electron effects, cell-to-cell interference, and high E-fields under 20 nm design rule. 3D NAND flash cell was developed to overcome many problems for 2D NAND cell. Also, it has continued to deliver and even accelerate the NAND scaling trends that the data industry demands. This is in part due to its larger gate area and improved electrostatics of the Gate All Around architecture using the thin poly-silicon channel. It has not only improved the cell characteristics such subthreshold swing and current but also reduced cell interference. As a result, the 3D NAND flash with superior performance has been currently enabled for three and four bit per cell to become main stream. 3D NAND architectures adapted "poly-Si channels," "word line replacement for metallization," and "plug etching process." In addition, to overcome the issue of peripherals taking up too large an area and too high a percentage of the total die size, a few different architectures were proposed. The peripheral circuit (CMOS) can be under array and another alternative is to build the peripheral circuits on a different CMOS wafer and then bond the memory wafer with the CMOS wafer using wafer-to-wafer microbonding, termed CMOS bonded array. Although the two architectures have many advantages for NAND cell, they still are suffering the degradation of read performance due increased BL RC delay. As NAND stack increases, it should be more challenge due to higher stack. In this paper, the new structure was proposed using NC-vTFT (NAND Cell-vertical TFT) on cell array in vertical NAND flash memory, for the first time. It will be very promising structure to improve RC delay as NAND cell stack increases.

Keywords: 3D NAND flash, NC-vTFT, COA structure, RC delay

1. Introduction

NAND flash memory is one of the most important nonvolatile memory devices that can hold programmed data without a power supply. With the wide spread of the portable equipment in audio/video fields such as MP3 players, digital cameras, and still mobile phone, the demand for low-cost and high-density flash memory has increased dramatically. NAND FLASH memory has dramatically increased density and reduced cost per bit which has driven creation of exciting new storage products over the years. These applications commonly need solid-state mass storage devices that feature high-density, low-cost, low power, nonvolatile, and portability. 2D NAND flash memory can easily satisfy the above needs. However, 2D NAND flash cells were unable to continue scaling due to several physical limitations including few electron effects, cell-to-cell interference, and high E-fields under 20 nm design rule. 3D NAND flash cell was developed to overcome many problems for 2D NAND cell. Recently, various 3D NAND flash memories such as stacked memory array transistor [1, 2], P-BiCS [3–5], TCAT [6, 7], V-NAND with Selective Epitaxial Gate (SEG) [8–11], and vertical gate [12, 13], which consists of the thin film poly-silicon (poly-Si) channel [14–17], have been introduced to be the most promising near-term solution to overcome scaling challenges in conventional planar NAND flash memories [18–23]. However, the side array and peripheral circuits in 3D NAND memory are like a ranch house in a crowded metropolitan downtown, where land is very precious. As the memory buildings grow taller, the peripheral circuits take a higher percentage of the total die size. As a result, 3D NAND scaling cost benefits are reduced accordingly [24, 25]. To find out the solutions for the issue of peripherals taking up too large an area and too high a percentage of the total die

***Corresponding author:** Daewoong Kang, Department of Next Generation Semiconductor Convergence and Open Sharing System, Seoul National University, Republic of Korea. Email: freekite@snu.ac.kr

Figure 1
(a) Existing CUA structure, (b) proposed COA structure to improve BL RC delay,
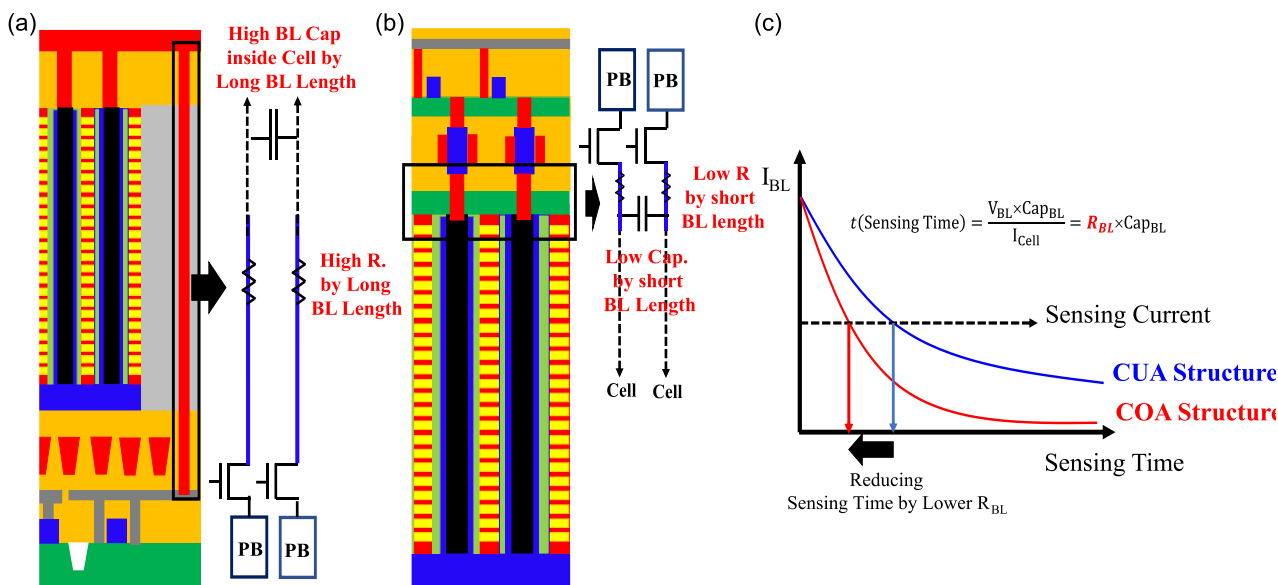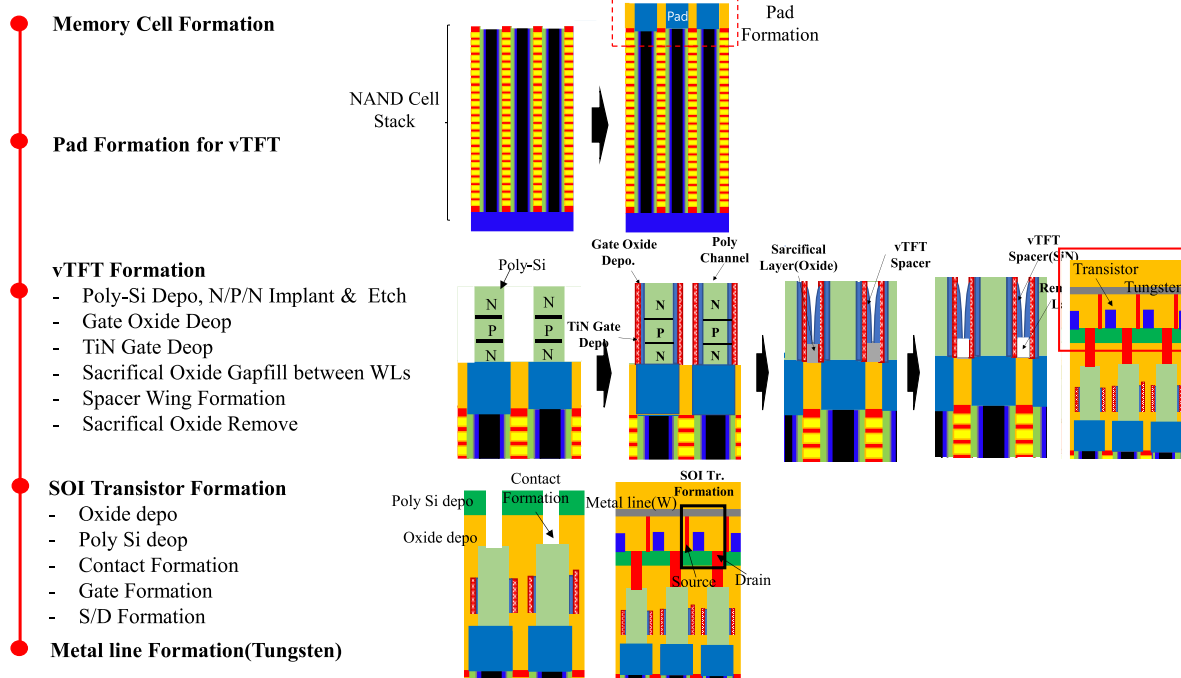**(c) bit line (BL) sensing schematic for CUA and COA**

Figure 2
Process flow schematic for proposed COA structure

size, few different architectures were explored. As shown in Figure 1(a), the peripheral circuit (CMOS) can be under array (CUA). Another alternative is to build the peripheral circuits on a different CMOS wafer and then bond the memory wafer with the CMOS wafer using wafer-to wafer microbonding, termed as CMOS bonded array (CBA) [26, 27] to improve the performance of CMOS transistors. Although both architectures have many advantages for NAND flash cell, they still are suffering from the degradation of read performance by increased BL RC delay as shown in Figure 1(a). As the height of 3D NAND flash stack recently increases by 232 layers, it should be more challenging due to higher stack [28–30]. In this

paper, we proposed new NAND flash cell structure using the vertical TFT (NC-vTFT) to improve the read and program performance through using reduced Bit line RC delay.

2. Process Flow and Simulation

2.1. Process flow for structure

Figure 1(a) shows the CUA structure is suffered by RC delay of Equation (1) due to increased BL (Bit Line) length as the height of NAND stack recently increases. Compared to Figure 1(a), the proposed structure can improve the RC delay as shown in Figure 1(b) [28, 31, 32].

$$t = \frac{V_{BL} \times Cap_{BL}}{I_{Cell}} = R_{BL} \times Cap_{BL} \tag{1}$$

It is because that BL resistance would be largely decreased by shorter bit line length of CMOS structure on cell array (COA). It can be explained by Equation (1) as function of BL voltage (V_{BL}) and BL capacitance (Cap_{BL}) and NAND cell current (I_{cell}) as shown in Figure 1(c). Figure 2 shows the process flow to fabricate the

COA structure. Firstly, NAND flash cells are fabricated using existing 3D NAND flash process flow TCAT [6, 7], V-NAND with SEG [8–11], and vertical gate [12, 13], and vTFT(vertical Thin-Film-Transistor) is used for a high-voltage transistor to control the program and erase operations with vertical channel on NAND cell structure [33]. The air gap process was applied for vTFT as shown in Figure 2 [34]. After that CMOS transistors can be fabricated using SOI or Fin-FET transistor on vTFT. SOI transistor was introduced in this paper.

2.2. Simulation for structure

Figure 3 shows the simulation structure that fabricated (1) SOI transistor, (2) vTFT, and (3) flash cell using Athena Silvaco TCAD Tool based on the process flow proposed in Figure 2. The detailed device parameters of simulation structure are listed in Table 1.

3. Results and Discussion

3.1. SOI transistor characteristics

Figure 4(a) and (b) show the secured I_d-V_g and I_d-V_d characteristics depending on channel boron doping and gate voltage for transistor with SOI, respectively. It was confirmed that they are normally operated. However, as the arsenic (As) implant energy increases for the drain doping, I_d abruptly decreases as shown in Figure 5(a). It is because of the higher drain resistance and less short channel effect in Figure 5(b) by deeper the arsenic doping profile in Figure 5(c).
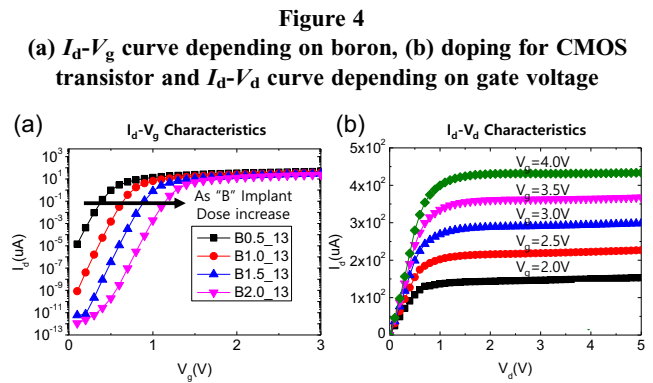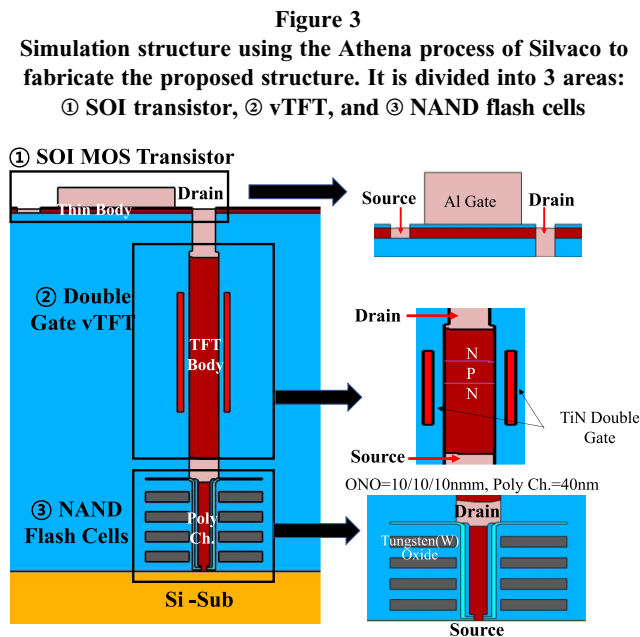
Figure 3
Simulation structure using the Athena process of Silvaco to fabricate the proposed structure. It is divided into 3 areas: ① SOI transistor, ② vTFT, and ③ NAND flash cells

Figure 4
(a) I_d-V_g curve depending on boron, (b) doping for CMOS transistor and I_d-V_d curve depending on gate voltage

Table 1
Detailed Spec. for simulation

	Source/Channel/Drain Implant Dose and Energy	Gate or WL Length (um)	SOI /vTFT/Cell Poly Thickness (nm)
SOI Transistor	Source: As $1 \times 10^{15}/cm^2$, 10 KeV Channel: B 1E13, 10 KeV Drain: As 1.0E15, 10 KeV	0.4	Thin Body Thickness=20 Gate Oxide=7
vTFT	Source: Ph $4 \times 10^{13}/cm^2$, 1000 KeV Channel: B $1 \times 10^{13}/cm^2$ 180 KeV Drain: Ph $1 \times 10^{15}/cm^2$ 60 KeV	1.0	TFT Body Thickness=100 Gate Oxide=20
NAND Cell	Source: Doped Poly Ph $10^{21}/cm^3$ Channel: Doped Poly B $4 \times 10^{17}/cm^3$ Drain: As 1E15, 50KeV	0.05 (Space=0.05)	Poly Ch. Thickness= 40 Oxide/Nitride/Oxide =10/10/10

Figure 5
(a) Linear scale and (b) log scale I_d-V_g curve depending on As implant energy, (c) doping profile depending on As implant energy
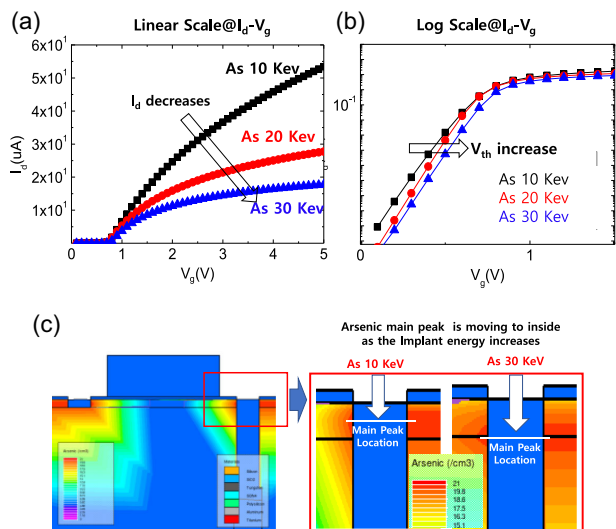

Figure 6
(a) Detailed process flow for proposed vTFT structure. (b) L_{eff} of vTFT for Ph implant energy depending on Ph implant dose. (c) Channel length depending on Ph energy
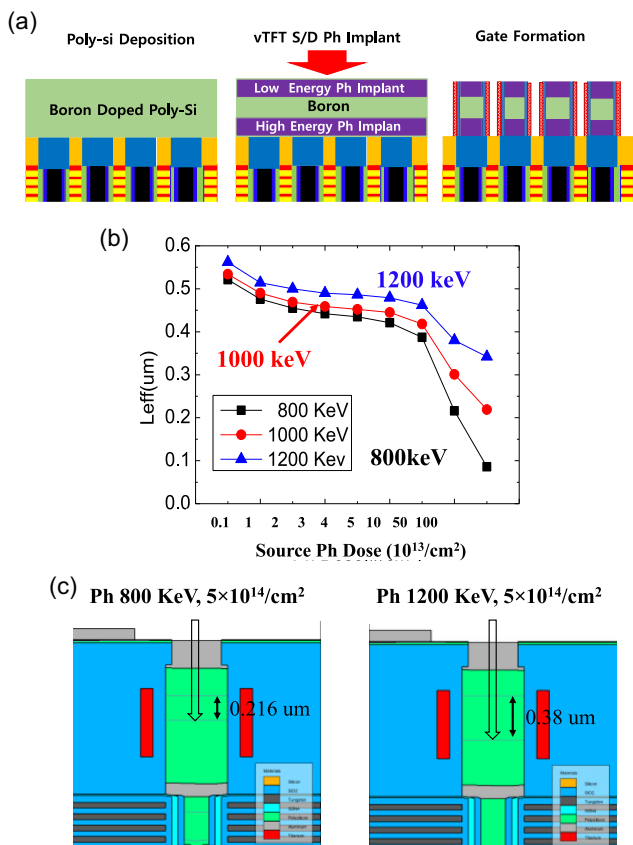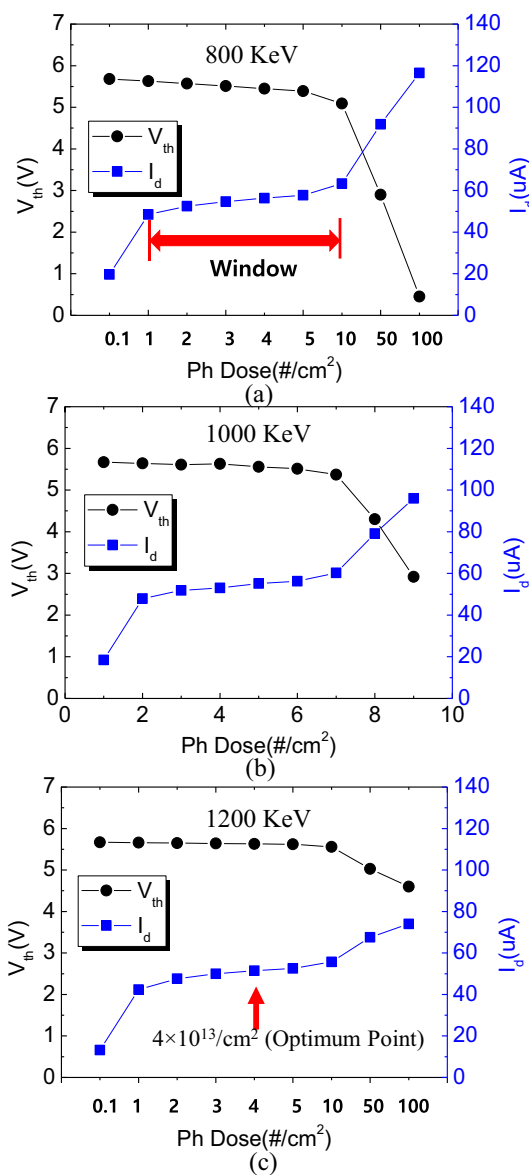

Figure 7
V_{th} and I_d characteristics depending on Ph implant dose between (a) 800 Kev, (b) 1000 KeV, and (c) 1200 KeV

3.2. vTFT transistor characteristics

Figure 6(a) describes the detailed process flow to fabricate vTFT. Figure 6(b) shows the results to optimize condition for phosphorous (Ph) implant energy and dose to form the source side of vTFT. As the Ph implant energy decreases, the results show the short channel effect as shown in Figure 6(c). Figure 7(a), (b), (c) show the process window of Ph dose for V_{th} and I_d. From this result, 4×10^{13}/cm^2 dose can be candidate as optimal value because it is located at middle point of window. In addition to vTFT characteristics depending on Ph implant energy and dose condition, the NAND flash cell characteristics should be considered as well because the cell V_{th} and I_d variation occurs by Ph penetrating to cell area as shown in Figure 8(a) and 8(b). It was explained in detail in chapter 3.3 NAND Flash cell characteristics.

Figure 8
(a) Cell V_{th} at WL2 for 4×10^{13} and 1×10^{14} Ph dose depending on Ph implant energy to fabricate vTFT and (b) I_d depending on cell V_{th} at WL = 2 for 4×10^{13} and 1×10^{14} Ph dose at Ph implant energy = 1000 KeV to fabricate vTFT

Figure 10
(a) I_d-V_g curve at WL2 depending on Ph implant energy for 1200 KeV, 1400 KeV, and 1600 KeV. Channel length depending on implant energy: (b) 1200 KeV and (c) 1600 KeV
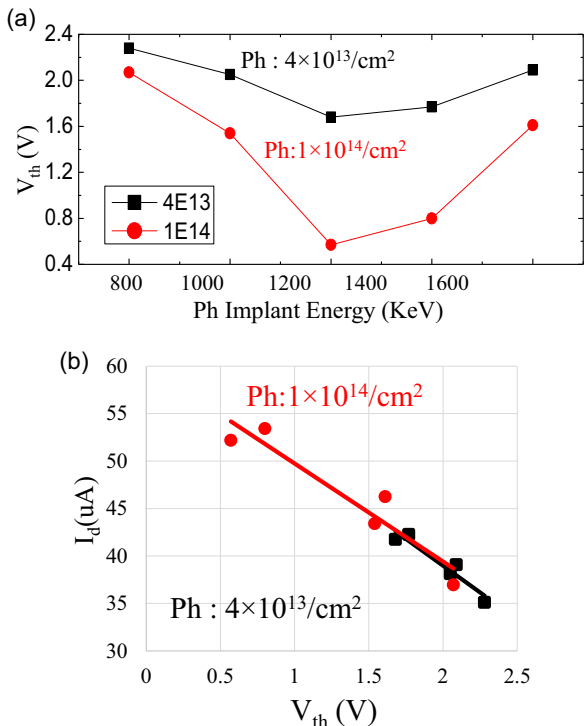

Figure 9
(a) I_d-V_g curve at WL2 depending on Ph implant energy for 800 KeV, 1000 KeV, and 1200 KeV. Channel Length depending on implant energy: (b) 800 KeV and (c) 1200 KeV
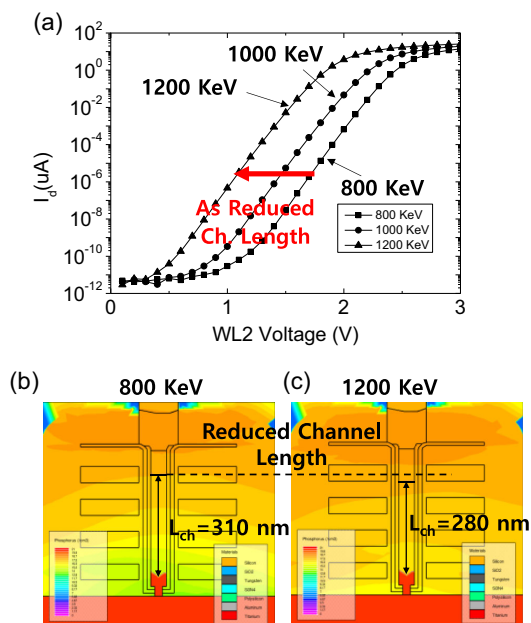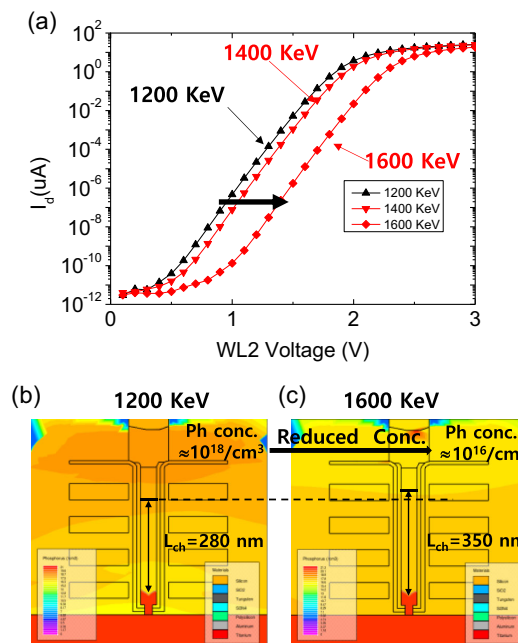

Figure 11
(a) Initial I_d-V_g depending on boron implant dose for cell channel. (b) Change of channel length depending on channel boron doping and inset shows the channel length in NAND flash cell
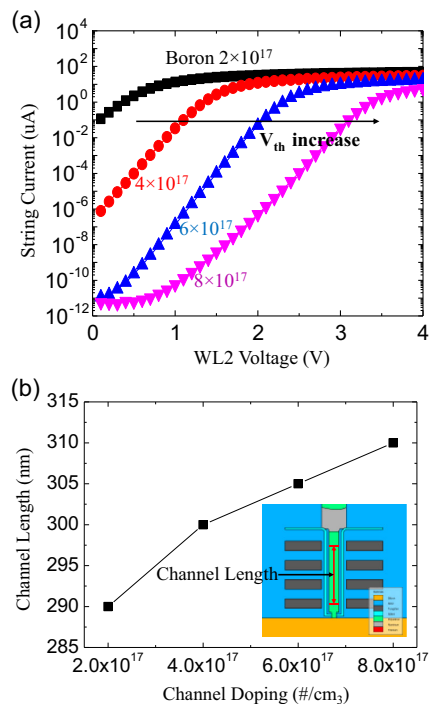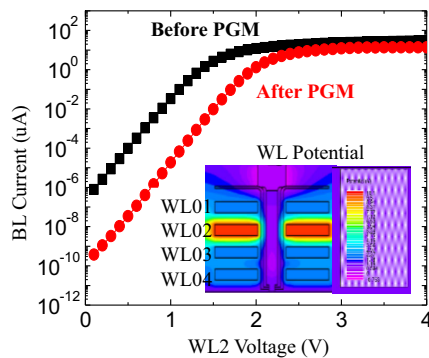

175

Figure 12
Program characteristics of cell at $V_{pgm} = 10V$ at WL = 2. Inset shows the WL potential at the program state

3.3. NAND flash cell characteristics

The high energy condition causes cell V_{th} to be larger variation that can be explained as two area. The high Ph implant energy between 800 and 1200 KeV makes the channel length reduced in Figure 9(a) because the main peak is formed at deeper location as shown in Figure 9(b) and (c). As Ph implant energy increases between 1200 and 1600 KeV, V_{th} becomes higher by increased channel length as shown in Figure 10(a). It is because that the main Ph peak deeply penetrates into inside NAND cell. It means the main Ph peak has passed the drain area as shown in Figure 10(b) and (c). Based on the result from Figures 7 and 8, Ph $4 \times 10^{13}/cm^2$ dose and 1000~1200 KeV energy can be proposed as the optimized conditions. Figure 11(a) shows the measured I_d-V_g and change of channel length depending on channel doping for NAND cell fabricated with optimized vTFT implant condition ($4 \times 10^{13}/cm^2$ dose and 1000 KeV energy). In Figure 11(b), the short channel effect is observed as the boron doping is lower in NAND cell channel. Additionally, it was confirmed that the program of WL02 in NAND cells is operated normally as shown in Figure 12.

4. Conclusion

Recently, a few different architectures have been proposed to overcome the issue of peripherals taking up too large an area and too high a portion of the total die size. One of them is the peripheral circuit (CMOS) can be under array (CUA) and another is to build the peripheral circuits on a different CMOS wafer and then bond the memory wafer with the CMOS wafer using wafer-to wafer micro bonding, termed as CMOS bonded array (CBA). Although the two architectures have many advantages for NAND cell, they still are suffering from the degradation of read performance due increased BL RC delay. As 3D NAND stack recently increases by 232 layers, it should be more challenging such as the degradation of RC delay due to higher stack height. Accordingly, 3D NAND flash is severely suffering from the degradation of read performance due to RC delay of bit line by higher stack height. In this paper, the COA structure using NC-vTFT was proposed to reduce the length of bit line for the first time. The COA structure consists of the SOI transistor, vTFT transistor, and 3D NAND cell with 4 layers. It was successfully fabricated using proposed process flow and the best Ion implantation conditions with Athena process simulation of Silvaco. The best process conditions were found out through the

various process split conditions because the thickness of each layer gives the impact on the doping profile to operate the transistor and NAND flash cells. As a result, the optimized process condition for Ion implantation ($4 \times 10^{13}/cm^2$ dose and 1000 KeV energy) to operate the transistors and 3D NAND flash cells was secured. Also, it was finally confirmed that Program and Read for 3D NAND flash cell was normally operated.

Conflicts of Interest

The authors declare that they have no conflicts of interest to this work.

Data Availability Statement

Data are available on request from the corresponding author upon reasonable request.

Author Contribution Statement

Hyowon Kang: Conceptualization, Formal analysis, Investigation, Writing – original draft, Writing – review & editing, Visualization. **Daewoong Kang:** Conceptualization, Methodology, Software, Validation, Formal analysis, Investigation, Resources, Data curation, Supervision, Project administration.

References

[1] Choi, E. S., & Park, S. K. (2012). Device considerations for high density and highly reliable 3D NAND flash cell in near future. In *International Electron Devices Meeting*, 9.4.1–9.4.4. https://ieeexplore.ieee.org/abstract/document/6479011

[2] Park, S. K. (2015). Technology scaling challenge and future prospects of DRAM and NAND flash memory. In *2015 IEEE 7th International Memory Workshop*, 1–4.

[3] Tanaka, H., Kido, M., Yahashi, K., Oomura, M., Katsumata, R., Kito, M., . . . , & Nitayama, A. (2007). Bit cost scalable technology with punch and plug process for ultra high density flash memory. In *IEEE Symposium on VLSI Technology*, 14–15.

[4] Komori, Y., Kido, M., Kito, M., Katsumata, R., Fukuzumi, Y., Tanaka, H., . . . , & Nitayama, A. (2008). Disturbless flash memory due to high boost efficiency on BiCS structure and optimal memory film stack for ultra high density storage device. In *2008 IEEE International Electron Devices Meeting*, 1–4.

[5] Nitayama, A., & Aochi, H. (2011). Vertical 3D NAND flash memory technology. *ECS Transactions*, *41*(7), 15.

[6] Jang, J. H., Kim, H. S., Cho, W. S., Cho, H. S., Kim, J. H., Shim, S. I., . . . , & Lee, W. S. (2009). Vertical cell array using TCAT (Terabit Cell Array Transistor) technology for ultra high density NAND flash memory. In *2009 Symposium on VLSI Technology*, 192–193.

[7] Cho, W. S., Shim, S. I., Jang, J., Cho, H., You, B., Son, B., . . . , & Chung, C. (2010). Highly reliable vertical NAND technology with biconcave shaped storage layer and leakage controllable offset structure. In *2010 Symposium on VLSI Technology*, 173–174.

[8] Kang, J. K., Lee, J., Yim, Y., Park, S., Kim, H. S., Cho, E. S., . . . , & Song, J. (2021). Highly reliable cell characteristics with CSOB (Channel-hole Sidewall ONO Butting) scheme for 7th generation 3D-NAND. In *IEEE International Electron Devices Meeting*, 10.1.1–10.1.4.

[9] Park, J. W., Kim, D., Ok, S., Park, J., Kwon, T., Lee, H., . . . , & Jin, K. W. (2021). 30.1 A 176-stacked 512Gb 3b/Cell 3D-NAND flash with 10.8Gb/mm^2 density with a peripheral circuit under cell array architecture. In *IEEE International Solid-State Circuits Conference*, 422–423.

[10] Park, S., Lee, J., Jang, J., Lim, J. K., Kim, H., Shim, J., . . . , & Song, J. (2021). Highly-reliable cell characteristics with 128-layer single-stack 3D-NAND flash memory. In *2021 Symposium on VLSI Technology*, 1–2.

[11] Kang, D., Park, H., Kim, D. H., & Cho, I. H. (2023). Device characteristics of the select transistor in a vertical-NAND flash memory. *Japanese Journal of Applied Physics*, *62*(2), 024001. https://doi.org/10.35848/1347-4065/acb57e

[12] Yeh, T. H., Wu, C. J., Hu, C. W., Chen, W. C., Lue, H. T., Shih, Y., . . . , & Lu, C.-Y. (2015). A new string decoding scheme for enhancing array block efficiency of vertical gate type (VG-Type) 3-D NAND. *IEEE Electron Device Letters*, *36*(4), 330–332.

[13] Chen, C. P., Lue, H. T., Chang, K. P., Hsiao, Y. H., Hsieh, C. C., Chen, S. H., . . . , & Lu, C. Y. (2012). A highly pitch scalable 3D vertical gate (VG) NAND flash decoded by a novel self-aligned independently controlled double gate (IDG) string select transistor (SSL). In *2012 Symposium on VLSI Technology*, 91–92.

[14] Hatalis, M. K., & Greve, D. W. (1988). Large grain polycrystalline silicon by low? Temperature annealing of low? Pressure chemical vapor deposited amorphous silicon films. *Journal of Applied Physics*, *63*(7), 2260–2266.

[15] Chen, H. L., & Wu, C. Y. (1998). An analytical grain-barrier height model and its characterization for intrinsic poly-Si thin-film transistor. *IEEE Transactions on Electron Devices*, *45*(10), 2245–2247.

[16] Kim, B. O., Lim, S. H., Kim, D. W., Nakanishi, T., Yang, S. R., Ahn, J. Y., . . . , & Kang, C. J. (2011). Investigation of ultra thin polycrystalline silicon channel for vertical NAND flash. In *International Reliability Physics Symposium*, 2E.4.1–2E.4.4.

[17] Park, H., Lee, I., Cho, I. H., & Kang, D. (2023). Improvement of cell characteristics using controlling the current path in 3D NAND flash. *Japanese Journal of Applied Physics*, *62*, SC1021. https://doi.org/10.35848/1347-4065/acaa41

[18] Hong, S. (2010). Memory technology trend and future challenges. In *2010 International Electron Devices Meeting*, 12.4.1–12.4.4.

[19] Lee, S. (2012). Scaling challenges in NAND flash device toward 10 nm technology. In *IEEE 4th International Memory Workshop*, 1–4.

[20] Park, Y. W., & Lee, J. D. (2013). Device considerations of planar NAND flash memory for extending towards sub-20 nm regime. In *IEEE 5th International Memory Workshop*, 1–4.

[21] Kar, G. S., Breuil, L., Blomme, P., Hody, H., Locorotondo, S., Jossart, N., . . . , & van Houdt, J. (2012). Ultra thin hybrid floating gate and high-k dielectric as IGD enabler of highly scaled planar NAND flash technology. In *2012 International Electron Devices Meeting*, 2.2.1–2.2.4.

[22] Breuil, L., Blomme, P., Tan, C. L., Lisoni, J. G., Souriau, L., Zahid, M. B., . . . , & van Houdt, J. (2014). Integration of a multi-layer inter-gate dielectric with hybrid floating gate towards 10 nm planar NAND flash. In *2014 IEEE 6th International Memory Workshop*, 1–4.

[23] Hsu, T. H., Lue, H. T., Lai, E. K., Hsieh, J. Y., Wang, S. Y., Yang, L. W., . . . , & Lu, C. Y. (2007). A high-speed BE-SONOS NAND flash utilizing the field-enhancement effect of FinFET. In *2007 IEEE International Electron Devices Meeting*, 913–916.

[24] Li, Y. (2020). 3D NAND memory and its application in solid-state drives: Architecture, reliability, flash management techniques, and current trends. *IEEE Solid-State Circuits Magazine*, *12*(4), 56–65.

[25] Jung, W., Kim, H., Kim, D. B., Kim, T. H., Lee, N., Shin, D., . . . , & Hur, S. H. (2024). 13.3 A 280-layer 1Tb 4b/cell 3D-NAND flash memory with a 28.5Gb/mm^2 areal density and a 3.2GB/s high-speed IO rate. In *IEEE International Solid-State Circuits Conference*, 236–237.

[26] Tagami, M. (2023). CMOS directly bonded to array (CBA) technology for future 3D flash memory. In *International Electron Devices Meeting*, 1–4.

[27] Kobayashi, S., Tashiro, K., Minemura, Y., Nakagami, K., Arita, K., Oohashi, T., . . . , & Sato, M. (2023). High peformance 3D flash memory with 3.2Gbps interface and 205MB/s program throughput based on CBA (CMOS Directly Bonded to Array) technology. In *International Electron Devices Meeting*, 1–4.

[28] An, H., Chun, J. Y., Park, H. K., & Jung, S. O. (2021). All-bit-line read scheme with locking bit-line and amplifying sense node in NAND flash. *IEEE Access*, *9*, 28001–28011.

[29] Song, J., Shim, J. M., Kim, B., & Song, Y. H. (2024). Concave and convex structures for advanced 3-D NAND flash memory technology. *IEEE Transactions on Electron Devices*, *71*(4), 2810–2814.

[30] Park, S. H., Yoo, H. N., Yang, Y., Kim, J. J., & Lee, J. H. (2024). Reliability improvement in vertical NAND flash cells using adaptive incremental step pulse programming (A-ISPP) and incremental step pulse erasing (ISPE). *IEEE Transactions on Electron Devices*, *71*(3), 1834–1838.

[31] Sachdeva, A., Gupta, L., Sharma, K., & Elangovan, M. (2023). A CNTFET based bit-line powered stable SRAM design for low power applications. *ECS Journal of Solid State Science and Technology*, *12*(4), 041006.

[32] Lee, S., Lee, S. S., Kwon, O. S., Lee, K. H., Byeon, D. S., Kim, I. Y., . . . , & Suh, K. D. (2003). A 90-nm CMOS 1.8-V 2-Gb NAND flash memory for mass storage applications. *IEEE Journal of Solid-State Circuits*, *38*(11), 1934–1942.

[33] Kim, J. H., Kim, S., & Park, B. G. (2019). Double-gate TFET with vertical channel sandwiched by lightly doped Si. *IEEE Transactions on Electron Devices*, *66*(4), 1656–1661.

[34] Kang, D., Jang, S., Lee, K., Kim, J., Kwon, H., Lee, W., . . . , & Shin, H. (2006). Improving the cell characteristics using low-k gate spacer in 1Gb NAND flash memory. In *2006 International Electron Devices Meeting*, 1–4.